

# GEE based soil loss estimation in Eastern Tigray Zones, Ethiopia

Dr Fikre Tekulu,

[fikrebelay23@gmail.com](mailto:fikrebelay23@gmail.com)

Adigrat University

**Zubairul Islam**

Adigrat University

**Haftom Gebre**

Adigrat University

**Tadesse Hadgu**

Adigrat University

---

## Research Article

**Keywords:** RUSLE, GEE, Soil Erosion, OLS, Grouping Analysis

**Posted Date:** March 26th, 2024

**DOI:** <https://doi.org/10.21203/rs.3.rs-4141126/v1>

**License:**  This work is licensed under a Creative Commons Attribution 4.0 International License.

[Read Full License](#)

**Additional Declarations:** No competing interests reported.

---

## **GEE based soil loss estimation in Eastern Tigray Zones, Ethiopia**

***Abstract:** Soil loss and its geostatistical analysis was studied at the kebele level in Tigray. The method applied to estimate soil loss was the revised universal soil loss equation. Earth Engine's public data archive was used for data collection. The R factor was developed from the SM2RAIN-ASCAT (2007-2021) global daily satellite rainfall data, the K-factor was developed from USDA-3A1A1A\_M/v02 soil data, the C-factor was derived from MODIS/006/MOD13A2, and LS factor was derived from WWF Hydro SHEDS Hydrologically Conditioned DEM. By integrating all factor, the soil loss was obtained by the RUSLE model. Spatial Autocorrelation (Morans I) statistic was used to identify the pattern of soil loss and Ordinary Least Squares (OLS) linear regression was used to model a soil loss in terms of its relationships to R, K, LS, C, and P factors. The grouping analysis tool was used to Group kebele based on soil loss. The results indicate that the estimated average soil erosion is  $82760 \text{ t ha}^{-1} \text{ y}^{-1}$ . The pattern of soil loss at the kebele level was found highly clustered with a z-score of 23.39. The groping analysis tool divides the kebele into five categories to identify the cause of spatial variation of the soil loss in Tigray. Groups 1, 4 & 5 were found as in the outlier positions due to the high LS factor. The results deliver valuable information for decision-makers and planners to take suitable land administration measures to minimize the soil loss. It, therefore, indicates google earth engine is a significant platform to analyse the RUSLE model for evaluating and mapping soil erosion quantitatively and spatially.*

**Keywords:** RUSLE, GEE, Soil Erosion, OLS, Grouping Analysis.

## Introduction

Land degradation hinders people across the globe from ensuring food security. Around 1.05 billion people are currently food insecure (Kuria et al. 2018). This phenomena is likely to get worse with this trend of land degradation with the world's population expected to reach 9 billion by 2050 (Rockström and Falkenmark, 2015). It is caused by many factors of both natural and anthropogenic sources. Deforestation and soil erosion are among the major reasons of land degradation. While deforestation is caused by increased population and the subsequent need for agricultural expansion, soil erosion is caused by runoff (more than 90% is caused by water erosion) (Megerssa and Bekere 2019). The effects of land degradation might not be revealed over short period of time; it is however manifested gradually with a catastrophic draught and starvation (Tesfahunegn 2020).

Soil erosion has continuously been an issue for human creatures all through history (Demirci & Karaburun, 2012). Soil erosion by water is a serious global problem. Around 5 Mg ha<sup>-1</sup> of beneficial topsoil is misplaced in lakes and seas each year (Angima et al., 2003). Land degradation is a serious problem across Sub-Saharan Africa. More than sixty-five % of the land has degraded up to some extent from very low to high. (Sileshi et al., 2019). Therefore, a precise evaluation of soil loss caused by precipitation is basic for common and rural assets administration (CHEN et al., 2017). Evaluation of soil disintegration is valuable in arranging and preservation works in a basin or a region (Ganasri & Ramesh, 2016).

Ethiopia, a country is mostly hit by land deterioration that resulted in poverty, reduction in agricultural yield, food insecurity, loss of human life, loss of livestock etc. Around two billion tons of soil is eroded annually which is equivalent to loss of about 1 million tons of grains annually (Megerssa and Bekere 2019). Soil erosion has a direct effect on yield reduction of agricultural products by altering the physico-chemical properties of soil such as a change in soils organic matter, texture, soil water content, soil nutrient decline etc. which are all a determining factor for the growth of crops. Consequences of Soil erosion vary from nutrient losses at upper stream to sedimentation deposition downstream, declining soil fertility, and yield losses.

Soil erosion in Ethiopia is more common on the highlands (semi-arid areas) when compared to the low lands, which receive relatively adequate rainfall amount. Semi-arid areas are with low vegetation cover, high runoff & soil loss. Soil erosion rates are generally highly dependent on land use type and agro climatic zones. For instance, cultivated lands encounter higher erosion rate than grasslands. The Tigray region in northern Ethiopia is highlands that is severely prone to soil erosion. The main reasons are associated to mountainous topography, intense rainfall, lack of /little vegetation cover. Frequent soil erosion in the Tigray has occurred for decades, which made farming on old arable lands difficult, and farmers had to look for more marginal lands (Esser and Haile 2002).

Soil erosion is because of runoff produced during the summer short but intense rainfall in Tigray. Other activities that aggravate soil erosion are the clearing of forests for the sake of alternative fuel sources. In Tigray, only the urban areas that account 15%

of the its population have access to power. The rest 85% living in remote areas are deprived to energy and all they depend is on wood fuel. Besides, cow dungs and cover crops that are vital to soil fertility are again used as fuel source. This has a detrimental effect on the quality of soil. Expansion of cultivated land by clearing forests has degraded the condition of the soil and accelerated soil erosion. The hilly and steep slope areas in the region are the most vulnerable to erosion because of the topography, old farming techniques of conventional tillage, and over cultivation (Kaygusuz, 2011).

Most of researches conducted so far focus on mitigating soil erosion mainly on implementation of soil and water conservation programs (Biazin et al. 2012), integrated watershed management (Teka et al. 2020), water harvesting (Filho and de Trinchiera Gomez 2017; Nyssen et al. 2010), and conservation tillage (Zerssa et al. 2021) etc. this programs are meant to enhance food and cash production, improve soil fertility and improve small holder farming. Those programs have been implemented at both house hold and community level. Those measures, although are limited to only few areas in the region such as the case of Abraha with Atsebha have shown promising results (Tadesse, Gebrelibanos, and Geberehiwot 2016). Soil and water conservation programs have the capacity to reverse erosion by reducing slope length, building a small retention basin to accumulate sediment and runoff, reducing water overland flow or water erosion (Vancampenhout et al. 2006).

However research on the estimation of soil losses in at regional or zonal level is very limited or insignificant. Despite being very limited, research conducted on soil loss estimation are conducted at plot scale and thus might not be used for estimating soil loss for large areas. Govers and Moeyersons (2005), conducted research on soil loss estimation at a plot scale on stone bunds, which are commonly, applied soil conservation technique by comparing plots with and without stone bunds. They found that mean annual soil loss estimated from sheet and rill erosion was 57 ton/ha/yr. no research has been conducted for estimating soil loss for larger areas at wereda level (the second administration unit in the region). Another study conducted on enclosure areas.

Estimating the rate of soil erosion for a larger area is however very essential element that should have been prioritized before the implementation of soil conservation works. It helps to quantify the amount of soil lost and the resulting decline in economy both at regional and country level. 2 billions of soil loss is equivalent to a loss of about 1 million ton of grains. Assessment of soil erosion at wider scale can help on the planning and design of agricultural policy and strategies in the region. It can help categorize areas from the most degraded areas to areas with less erosion hence, to identify areas of focus. Thus answers the question, which areas need to be prioritized during soil conservation programs. This can facilitate the implementation and adoption more soil conservation works.

Soil erosion models play a key role at forecasting the impacts of landscape alterations on both socio economic and environmental sustainability. They help estimate soil loss and runoff from different land use, gives information about the present and future erosion and scenario analysis. They also serve as a guideline for policies and strategies linked to soil water conservation.

There exist several erosion models have been developed so far including the RUSLE model (revised universal soil loss equation), soil & water assessment tool (SWAT), AGNPS (Agricultural non-point source pollution), Euro SEM (European soil erosion

model), WEPP (water erosion predication project) etc. all with a common goal of sediment or soil loss estimation but mostly differ on the input parameters, whether an empirical, conceptual or physical based models are used for simulating the model, process and complexity of the model etc. (Moges and Bhat 2017). The selection on a suitable model is highly dependent on the aim of the study, catchment properties, data availability, model accuracy and simplicity (Luvai, Obiero, and Omuto 2022). For instance, RUSLE, is a commonly applied empirical soil erosion model designed for areas with hilly topography. Empirical models such as RUSLE are easy to use models, which can even be applied in case of limited input data (P.U. et al. 2017). It has been applied by (Bagegnehu, Alemayehu, and Nigatu 2019; Ganasri and Ramesh 2016; K., F., and O. 2020; Mekuria et al. 2009; Moges and Bhat 2017). The USLE model that was developed by Wischmeier and Smith, (1978) was first designed to estimate soil loss for sloppy areas where parameters like slope length and slope steepness were used to determine the impact of terrains on erosion. This model was later on improved to a RUSLE model which made it applicable for more land use types such as crop land, range lands, forest lands, and steep areas (P.U. et al. 2017; Van Remortel, Hamilton, and Hickey 2001). The RUSLE model have been applied enormously for the last 20 year and continued to be the most preferred soil erosion model used to estimate sheet & rill erosion caused by runoff (Borrelli, Alewell, and Alvarez 2021).

Nowadays, including remote sensing in to existing soil loss modeling has become a popular technique in areas of hydrology, agriculture, soil science etc. for simulating events and processes with the help of spatial analysis (Ahmed Harb Rabia 2012). GIS based water erosion model can help examine spatial pattern of soil attrition, its transfer and deposition as well as its effect on the landscape formation (Mitasova et al. 2013). Combination soil erosion models, with remote sensing data such can identify highly erosive areas on a cell-by-cell basis with input from digital elevation model (Ganasri and Ramesh 2016).

Erosion models, depending on the catchment scale for which they are designed need different spatial dataset resolutions. For instance, a spatial resolution up sub meter is needed for hill slope scale where sheet and rill erosion is dominant. A watershed/catchment scale model on the other hand requires a spatial resolution of up to 10 meter and includes large gullies. Regional scale modeling are macroscale catchments of up to thousands of km<sup>2</sup>, thus require a spatial resolution from 30 meter to hundred meters (Mitasova et al. 2013). Some of the papers that combined GIS and one of the RUSLE erosion models (Ahmed Harb Rabia 2012; Bagegnehu et al. 2019; Borrelli et al. 2021; K. et al. 2020; Luvai et al. 2022; Moges and Bhat 2017).

The USLE (Wischmeier & Smith, 1965, 1978) was formulated to predict the long term twenty years mean soil loss per year from field size areas using five factors focusing on the effect of climate, especially rainfall, soil, topography, cropping, and soil conservation activities (Kinnell, 2014). The RUSLE has also expanded its uses to different conditions (Lu & others. 2004). RUSLE is one of the most widely used (Abu Hammad & others. 2004) soil erosion models worldwide (Tanyaş et al., 2015).

The rainwater erosivity factor denotes the kinetic energy of raindrops, which could affect the steadiness of soil aggregates (Yue et al., 2020) and enhance soil loss (Hateffard et al., 2021). The soil erodibility calculate  $k$  appears the resistance of soil against disintegration due to the effect of a raindrop and the rate and sum of runoff created for that precipitation impact, under a standard condition (Ghosal & Das

Bhattacharya, 2020). Climate change could further accelerate the process of soil loss, in consequence of climate change, an increase in local flash floods and soil erosion intensity would be expected (Fiener & others. 2013). As the temporal resolution of precipitation measurement declines, calculated precipitation erosivity declines (Yue et al., 2020).

The soil erodibility variables for showing soil erosion are stated as the k variable in the widely used soil erosion model the USLE and its revised version RUSLE (Panagos et al., 2014). The soil erodibility variable (K) denotes the power of soil against disintegration because of the effect of the drop of the rain and the rate and amount of run-off developed for that precipitation effect, under a standard condition (Ghosal & Das Bhattacharya, 2020). The utmost problem with soil erosion modeling at greater spatial scales is the absence of data on soil characteristics.

When utilizing the USLE or RUSLE, the impacts of terrain on soil disintegration are evaluated by the steepness & length of the slope constituents of the dimensionless LS factor, where LS is one of five variables (R, K, LS, C, and P) that are multiplied all to calculate the normal yearly soil removal per unit area (Van Remortel et al., 2001). The LS figure contains the slope length figure (L) and the slope factor (S). It is broadly accepted that slope length is the trickier portion. The improvement of GIS permits for programmed extraction of slope length from high-resolution DEMs, hence an inefficient manual process is avoided (Liu et al., 2015). The LS-factor was initially created for slopes less than 50% slant and has not been tried for more extreme slopes. To overcome this confinement, (Schmidt et al., 2019) adjusted both components slant length L and slant steepness S for conditions tentatively watched at Swiss elevated prairies.

Greenery cover is seen among the foremost critical saving measures for controlling soil disintegration caused by rainfall. a lot of work has been published related to the fact that vegetation cover is more sensitive, down to earth, it is possible to calculate normalized difference vegetation list (NDVI) for calculating “cover management (C) factor” within the Changed Universal Soil Loss Condition (RUSLE), the foremost commonly recognized soil disintegration prediction show around the world (Vatandaslar & Yavuz, 2017). Land cover, a vital calculation for checking changes in land use and disintegration chance, has been broadly checked and assessed by vegetation indices (Durigon et al., 2014).

The conservation practice variable (P) of the RUSLE stays to a great extent hazy (Tian et al., 2021). The variables utilized in these models were ordinarily assessed or calculated from field estimations. The strategies of evaluating soil misfortune based on disintegration plots have numerous confinements in terms of fetched, representativeness, and unwavering quality of the coming about information. They cannot give the spatial distribution of soil disintegration loss due to the limitation of constrained tests in complex situations. So, mapping soil disintegration in large zones is regularly exceptionally troublesome utilizing these conventional strategies (Lu et al., 2004). In any case, the utilization of farther detecting and geographical information framework (GIS) procedures makes soil disintegration estimation and its spatial dispersion attainable with reasonable costs and way better precision in bigger zones. The RUSLE has been adopted in a Geographical data information system (Kouli et al., 2009). Spatial analysis is a part of geography, which has a varied and inclusive ability that comprises the basic visual investigation of maps and imagery, computational

analysis of areal patterns, finding best routes, point selection, and advanced forecast modeling (ESRI, 2013).

GIS is included in many disciplines have been used significantly in combinations of many different models, such as RUSLE, to predict soil disintegration (Demirci & Karaburun, 2012). Spatial statistics were somehow developed by Pearson and Fisher, but their modern appearance is mainly due to Whittle, Moran, and Geary (Waters, 2012).

Using GIS models any one can forecast soil removal risk, based on the level of erosion at a variety of levels (Evans & Boardman, 2016), but field-based assessments are very important for result validation. As we know the population is increasing day by day so the protection of soil has been a very significant task (CHEN et al., 2017).

The Geographers and GIS experts focus on the need of the land administrators and policy developers and they are more concerned with the spatial variation of soil removal risk than only numerical figures of soil erosion loss (Lu & others, 2004).

This research focuses on application of geostatistical analysis for estimating soil loss for Tigray. It had done by combining GIS data with the revised universal soil loss equation model (RUSLE).

### **Purpose of the work**

The purpose of this is; first, to predict the soil erosion using RUSLE; second, to predict the pattern of soil loss at the kebele level in Tigray Region; third, to exercise linear regression to understand the impact of variables of soil loss and the last to group the kebele based on soil loss estimation.

There have been relatively few regional studies in the Tigray regional state of Ethiopia on the use of RUSLE technologies for finding the kebele prone to more water erosion. Using Geostatistics, the current study tried to analyze the areal differentiation of soil loss due to rainfall in the study area.

### **Material and Methods**

#### **Study Area**

Eastern Tigray Zone is located in the northern part of Ethiopia and is composed of 18 woredas, with a total area of 6,392 km<sup>2</sup>. It is located between 13°32'59"N up to 14°40'56"N latitude and between 39°11'39"E up to 39°59'43"E longitude. Generally, this zone is bordered by Eritrea in the North, by the Central zone in the West, by the South Eastern in the South, and by the Afar regional State in the East.

#### **Topography of the Study Area**

The general topography of the influence area ranges from its lowest 148 meters above sea level up to 3,298 meters above sea level. Its mean elevation above sea level equals 2,225 meters. It is characterized by the local climate primarily 'degua', 'weyna degua' and 'kola.

### Climate of the Study Area

The climate is commonly defined as the weather average over a long period mostly used for 35 years. Climate includes the statistics of temperature, humidity atmosphere pressure, wind, and precipitation. However, the data is limited to temperature and rainfall. These two climatic elements of the course are the most important for both agriculture and hydrology.

In Eastern Tigray, as in other parts of the country, the climate is determined by latitudinal and altitudinal factors. Annual rainfall of the zone ranges from its minimum in Erob about 140 mm up to the highest in Saesie-Tsaeda-Emba about 672mm. Similarly, with regard to temperature, the lowest temperature is experienced in Ganta Afeshum including Adigrat about 6°C up to the maximum of about 30°C in Erob (Adigrat University, 2018).

Several land use types including forests, croplands, built-up area, and enclosure areas exist in Tigray. Typical soil types in the region include, lithosols, cambisols, acrisols, vertisols luvisols, xerosols regosols, arenosols, fluvisols rendzinas nitosols (Gebregziabher et al., 2009). Mixed farming system of crop farming with livestock production are typical farming practices in the region of which more than 90% of farming is practiced by small holder farming. (Zerssa et al., 2021). Agriculture is the mainstay economy in the region contributing to 60% of GDP. The main crops grown in in the region are barley, maize, wheat, sorghum, Teff (*Eragrostis tef*), along with leguminous crops: chickpeas, field peas, and horse bean. Sheep, goat, Cattle, beehives, and chicken are common livestock reared in the zone.

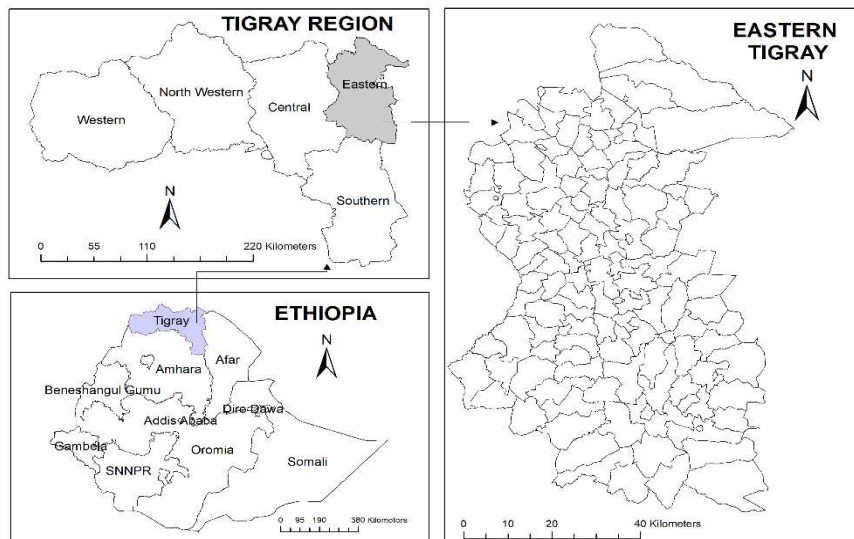


Figure 1 Study Area Map



## Workflow

RUSLE is fit for the soil loss estimation model that can be used at any level of region (Ganasri & Ramesh, 2016). The workflow implemented in this study is given in fig. 02.

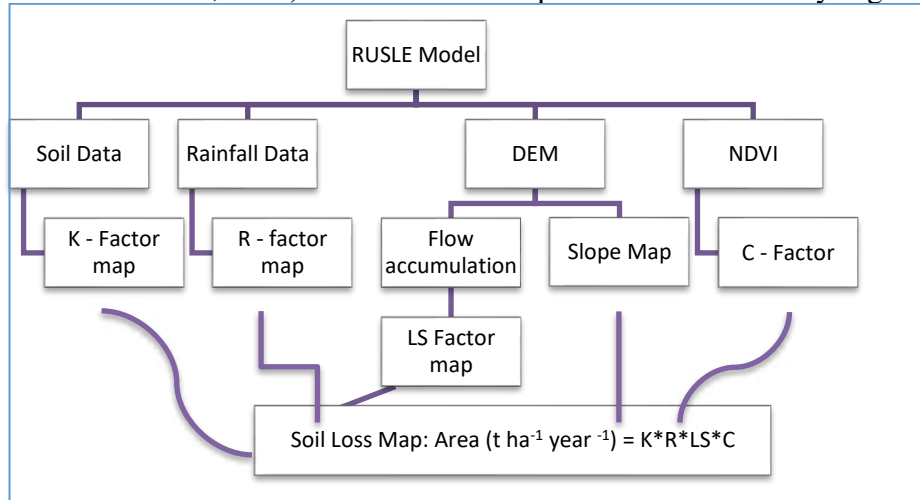


Figure 2 RUSLE Workflow chart

## Data Used

The source and type of data used are given in table 01.

## Data Processing

### 2.4.1 RUSLE

RUSLE, one of the foremost widely used models (Eq. 1), gives an idea of how to get the interaction between precipitation and soil erosion (Xu et al., 2013).

$$A = R * K * LS * C * P \quad (1)$$

where, R stands for precipitation runoff erosivity factor ( $\text{MJ} \cdot \text{mm} \cdot \text{km}^{-2} \cdot \text{h}^{-1} \cdot \text{month}^{-1}$ ); K is for the soil erodibility variable ( $\text{t} \cdot \text{km}^2 \cdot \text{h} \cdot \text{km}^{-2} \text{ MJ}^{-1} \cdot \text{mm}^{-1}$ ); LS is steepness and length of the slope factor (dimensionless); C is the factor for cover management (dimensionless); P is the erosion control practice factor (dimensionless, between 0 and 1) and A is the calculated soil loss ( $\text{t} \cdot \text{km}^{-2} \cdot \text{annum}^{-1}$ ).

**Rainfall factor (R):** For the monthly R, it is calculated according to daily data or monthly data.

$$R = 1.73 * 10^{(1.5 * \log(\frac{Pm^2}{Pa}) - 0.08188)} \quad (2)$$

Where R is the erosivity by rainfall in  $\text{MJ} \text{ in } \text{mm} / \text{ha } \text{h}^{-1} \text{ y}^{-1}$ , Pm is the precipitation in the month and Pa is the precipitation in a year.

Box 1 shows the Java script used in GEE to find the R factor.

```

var Precipitation_E_Tigray=
ee.Image("OpenLandMap/CLM/CLM_PRECIPITATION_SM2RAIN_M/v01")

var Annual_Precipitation_E_Tigray= Precipitation_E_Tigray.reduce(ee.Reducer.sum())

var Monthly_Precipitation_T E_igray=
ee.Image(10).pow(ee.Image(1.5).multiply(Precipitation_E_Tigray.pow(2).divide(Annual_Precipitation_E_Tigray).log10().subtract(-0.08188))).multiply(1.735)

var factorR = Monthly_Precipitation_Tigray.reduce(ee.Reducer.sum())

```

*Box 1 GEE code for rainfall erosivity factor (R)*

**Soil factor (K):** It can be assessed using soil's texture and organic data (Sharpley and Williams, 1990).

$$K = [0.2 + 0.3 * \exp - 0.0256 * SAN * (1 - SIL/100)] * [1 - \frac{0.25 * CLA}{CLA + \exp(3.72 - 2.95 * CLA)}] \quad (3)$$

where SAN is the sand percentage, SIL is the silt percentage and CLA is the clay percentage.

Box 2 shows the Java script used in GEE to find the factor of soil erodibility (K).

```

var sand = ee.Image("OpenLandMap/SOL/SOL_CLAY-WFRACTION_USDA-3A1A1A_M/v02").select('b0')

var silt = ee.Image('users/aschwantes/SLTPPT_I').divide(100)

var clay = ee.Image("OpenLandMap/SOL/SOL_SAND-WFRACTION_USDA-3A1A1A_M/v02").select('b0')

var morg = ee.Image("OpenLandMap/SOL/SOL_ORGANIC-CARBON_USDA-6A1C_M/v02").select('b0').multiply(0.58)

var sn1 = sand.expression('1 - b0 / 100', {'b0': sand})

var orgcar = ee.Image("OpenLandMap/SOL/SOL_ORGANIC-CARBON_USDA-6A1C_M/v02").select('b0')

var soil = ee.Image([sand, silt, clay, morg, sn1, orgcar]).rename(['sand', 'silt', 'clay', 'morg', 'sn1', 'orgcar' ])

var factorK = soil.expression(
'(0.2 + 0.3 * exp(-0.0256 * SAND * (1 - (SILT / 100)))) * (1 - (0.25 * CLAY / (CLAY + exp(3.72 - 2.95 * CLAY)))) * (1 - (0.7 * SN1 / (SN1 + exp(-5.51 + 22.9 * SN1))))',

```

*Box 2 GEE code for soil erosivity factor (K)*

**LS factor:** It is an accelerating factor for rainfall erosion. Moore (1985) developed the method of slope length. S is assessed by step coupling techniques (McCool. 1989; Liu.1994).

$$LS = (0.4 + 1) * (Flowacc * CellSize/22.13)^{0.4} * (\sin\theta/0.0896)^{1.3} \quad (4)$$

where LS is the horizontal length of the slope; Flowacc is the horizontal length of the slope  $\theta$  is the slope of DEM (Degrees). Box 3 shows the Java script used in GEE to obtain the LS factor.

```
var facc = ee.Image("WWF/HydroSHEDS/15ACC")
var dem = ee.Image("WWF/HydroSHEDS/03CONDEM")
var slope = ee.Terrain.slope(dem)
var ls_factors = ee.Image([facc,
slope]).rename(['facc','slope'])
var factorLS = ls_factors.expression(
'(FACC*270/22.13)**0.4*(SLOPE/0.0896)**1.3',
{
  'FACC': facc,
  'SLOPE': slope
})
```

*Box 3 GEE code for LS erosivity factor (LS)*

**C factor:** It is related to cover management, which was calculated from the NDVI (Eq. 5):

$$NDVI = (NIR - Red)/(NIR + Red) \quad (5)$$

Where *Red* & *NIR* are the wavebands of EMR.

The technique (Eq. 6) for the C factor was used because the CrA is dependent on NDVI & tropical climate conditions (Almagro et al., 2019).

$$CrA = 0.1 * ((-NDVI + 1)/2) \quad (6)$$

Box 4 shows the Java script used in GEE to obtain the C factor.

```
var ndvi_median = ee.ImageCollection("MODIS/006/MOD13A2").
median().multiply(0.0001).select('NDVI')
var factorC = ndvi_median.expression(
'0.1 * ((- NDVI + 1) / (2))', {
  'NDVI': ndvi_median, });
```

*Box 4 GEE code for cover management factor (C)*

**P factor:** The P-factor signifies comprehensive, overall effects of practices supporting conservation. It accounts for how surface environments distress flow paths and flow hydraulics. Presently, no major erosion control/support practices data of Tigray was available; henceforth it was given a value of 1.0 such that it had no effect on the design of soil loss.

#### 2.4.2 Geostatistical Analysis

To predict the pattern of soil loss at kebele level in Tigray the Spatial Autocorrelation (Global Moran's I) tool was used. This tool calculates spatial autocorrelation based on both location and values of the features simultaneously. The pattern may be dispersed, clustered, or random, it depends on the location and the attribute values of the features.

The Moran's I statistic for spatial autocorrelation is given as eq. 07 to 11.

$$I = \frac{n}{S_0} \frac{\sum_{i=1}^n \sum_{j=1}^n w_{i,j} z_i z_j}{\sum_{i=1}^n z_i^2} \quad (7)$$

Where  $z_i$  denotes the feature's attribute deviation from its average is the spatial weightage in between feature  $j$  and  $i$ ,  $n$  is all number of features, and  $S_0$  is the combination of all the spatial weights:

$$S_0 = \sum_{i=1}^n \sum_{j=1}^n w_{i,j} \quad (8)$$

The  $z_i$ -score for the statistic is computed as:

$$z_I = \frac{I - E[I]}{\sqrt{V[I]}} \quad (9)$$

Where:

$$E[I] = -1/(n - 1) \quad (10)$$

$$V[I] = E[I^2] - E[I]^2 \quad (11)$$

To meet the third research objective ordinary least square regression type was used (Eq. 12).

$$\gamma = \beta_0 + \beta_1 X_1 + \beta_2 X_2 + \beta_3 X_3 + \dots + \beta_n X_n + \varepsilon \quad (12)$$

Where  $\gamma$  is the dependent variable,  $\beta$  is coefficients, X is explanatory variables and  $\varepsilon$  is the random error.

To better understand how the factors are affecting the soil loss predictions Grouping Analysis tool was used to partition the kebele of Tigray (Eq. 13 & 14).

$$\begin{aligned} \text{Calinski – Harabasz pseudo F – statistic} & \quad (13) \\ & = (R^2/n_c - 1)/(1 - R^2/n - n_c) \end{aligned}$$

Where:

$$R^2 = \frac{SST - SSE}{SST} \quad (14)$$

In addition, SST is a reflection of between-group differences and SSE reflects within-group similarity:

$$SST = \sum_{l=1}^{nc} \sum_{k=1}^{ni} \sum_{j=1}^{nv} (V_{ij}^k - \bar{V}^k)^2 \quad (15)$$

$$SST = \sum_{l=1}^{nc} \sum_{k=1}^{ni} \sum_{j=1}^{nv} (V_{ij}^k - \bar{V}_l^k)^2 \quad (16)$$

Where

$n$  = the number of features

$n_i$  = the number of features in group  $t$

$n_c$  = the number of classes (groups)

$n_v$  = the number of variables used to group features

$V_{ij}^k$  = the value of the  $k^{\text{th}}$  variable of the  $j^{\text{th}}$  feature in the  $t^{\text{th}}$  group

$\bar{V}^k$  = the mean value of the  $k^{\text{th}}$  variable

$\bar{V}_l^k$  = the mean value of the  $k^{\text{th}}$  variable in group  $i$

### **3. Results**

#### **3.1 Precipitation runoff erosivity factor (R)**

The predicted map of the annual R factor is given in Fig. 03. The min. and max. R is found 178.24 to 4329.05 respectively. The mean annual R in Eastern Tigray zone is 2478 with a standard deviation of 1069.

#### **3.2 Soil erodibility factor (K)**

The predicted map of the annual R factor is given in Fig. 04. The min. and max. K is found at 0.245 to 0.3558 respectively. The mean annual K in Tigray is 0.27 with a standard deviation of 0.01.

#### **3.3 Slope length steepness factor (LS)**

The predicted map of the annual LS factor is given in Fig. 05. The min. and max. LS is found 00 to 318523 respectively. The mean annual K in Eastern Tigray zone is 3607 with a standard deviation of 9046.

#### **3.4 Cover management factor (C)**

The predicted map of the annual C factor is given in Fig. 06. The min. and max. C is found at 0.020 to 0.046 respectively. The mean annual C in Eastern Tigray Zone was found 0.04.

#### **3.5 Annual Soil Loss**

The estimated soil loss in Tigray is shown in Fig.07. The min. and max. soil loss is found 00 to 7425130 t ha<sup>-1</sup> year<sup>-1</sup> respectively. The mean annual K in Eastern Tigray Zone is 65677 t ha<sup>-1</sup> year<sup>-1</sup> with a standard deviation of 144121.

#### **3.6 Pattern of Soil loss at the kebele level**

The result of autocorrelation for pattern analysis is given in table 02 & Fig. 07, which, indicates soil loss at the kebele level is highly clustered ( $z = 3.94$ ).

#### **3.7 Standard Residuals of Annual soil loss Prediction**

Fig. 08 & 09 shows the map and histogram of Standard Residuals respectively. Table 03 & 04 shows the results of the model variables & OLS diagnostics. The multiple R<sup>2</sup> was obtained as 0.70 from the ordinary least squared (OLS) regression model.

#### **3.8 Groups of Annual soil loss Prediction**

Figure 10 & 11 shows the map of the groups of Annual soil loss Prediction & Parallel box plot chart respectively. Group numbers one and five are of special interest because of their outlier positions as shown in the Parallel box plot chart (Fig.10).

## **Discussion**

Eastern Tigray zone is a very zig zag region; different types of topography are found here. Many researchers have also assessed soil erosion in Eastern Tigray zone. However, very less work is done on soil erosion at Kebele level in Eastern Tigray zone based on GIS. Estimates of soil removal by water show significant variation at the kebele level, this variation is a result of the variation in the distribution of different types of the soil, high flow accumulation, variations in vegetation cover, and finally spatial variation of rainfall. The R factor; which shows the impact of rainfall was calculated based on reliable rainfall data with quality control. Data record provides better information, especially in Africa (Brocca & others 2019). The K factor that is modeled in this study is also based on the full soil properties currently available. The same soil data was used by other researchers such as Viscarra, E. N., & Baldock, J. A. in 2014. de Brogniez, D., Ballabio, C., Stevens, A., Jones, Montanarella, L., & van Wesemael, B. in 2015. The results are consistent with other scholars. Most areas of Tigray have a relatively small value of K. The vegetation data MOD13A2 used to calculate cover management was collected from the Google Earth engine archive. The same data has also been used by He et al., 2022; Wu et al., 2022; Chabot et al., 2022; He & others, 2022. The results were validated and published.

The OLS regression model was used to predict the significance of the factors; different tests are required to confirm the reliability of the OLS regression model. The modeled relationships are consistent because obtained statistic of Koenker is not statistically significant (p more than 0.005). The residuals show a Gaussian spatial pattern by the areal autocorrelation (Global Moran's I) analysis. Model predictions are unbiased because the Jarque-Bera Statistic test is also not statistically significant (p more than 0.01). There are no high intercorrelations among explanatory variables.

In the result of the grouping analysis Group, five has maximum mean soil loss, and this is primarily due to the high rainfall erosivity factor. The low soil loss in-group one is due to the low LS factor.

## **Conclusion**

Smart techniques such as the GEE interface were used for erosivity factors of R, LS, C and K. In general, it was found that the soil erosion is high due high rainfall and zigzag topography in the Eastern Tigray zone, which equates to heavy annual soil losses over this area. The kebele that suffers from severe soil erosion occurs in areas having higher rainfall, more slope length and steepness (LS) factors; therefore, these areas should be further studied. GEE is useful for the estimation of soil removal. As it can process data input at any level, RUSLE can provide quantitative estimates of long-term soil removal in Eastern Tigray.

## References

- Abu Hammad, A., Lundekvam, H., & Børresen, T. (2004). Adaptation of RUSLE in the eastern part of the Mediterranean region. *Environmental Management*, 34(6), 829–841. <https://doi.org/10.1007/s00267-003-0296-7>
- Adigrat University. (2018). Adigrat city structural plan preparation (2018–2028), unpublished material
- Ahmed Harb Rabia. (2012). GIS Spatial Modeling for Land Degradation Assessment in Tigray, Ethiopia. 161–166. <https://sites.google.com/site/aharbrabia/services>
- Almagro, A., Thomé, T. C., Colman, C. B., Pereira, R. B., Marcato Junior, J., Rodrigues, D. B. B., & Oliveira, P. T. S. (2019). Improving cover and management factor (C-factor) estimation using remote sensing approaches for tropical regions. *International Soil and Water Conservation Research*, 7(4), 325–334. <https://doi.org/10.1016/j.iswcr.2019.08.005>
- Angima, S. D., Stott, D. E., O'Neill, M. K., Ong, C. K., & Weesies, G. A. (2003). Soil erosion prediction using RUSLE for central Kenyan highland conditions. *Agriculture, Ecosystems and Environment*, 97(1–3), 295–308. [https://doi.org/10.1016/S0167-8809\(03\)00011-2](https://doi.org/10.1016/S0167-8809(03)00011-2)
- Bagegnehu, B., Alemayehu, M., & Nigatu, W. (2019). Geographic Information System (GIS) based soil loss estimation using Universal Soil Loss Equation Model (USLE) for soil conservation planning in Karesa Watershed, Dawuro Zone, and South West Ethiopia. *International Journal of Water Resources and Environmental Engineering*, 11(8), 143–158. <https://doi.org/10.5897/ijwree2018.0820..143-158>
- Biazin, B., Sterk, G., Temesgen, M., Abdulkedir, A., & Stroosnijder, L. (2012). Rainwater harvesting and management in rain fed agricultural systems in sub-Saharan Africa - A review. *Physics and Chemistry of the Earth*, 47–48, 139–151. <https://doi.org/10.1016/j.pce.2011.08.015>
- Borrelli, P., Alewell, C., & Alvarez, P. (2021). CO. March. <https://doi.org/10.31223/X5GS3T>
- Brocca, L., Filippucci, P., Hahn, S., Ciabatta, L., Massari, C., Camici, S., ... Wagner, W. (2019). SM2RAIN–ASCAT (2007–2018): global daily satellite rainfall data from ASCAT soil moisture observations. *Earth System Science Data*, 11(4), 1583–1601. <https://doi.org/10.5194/essd-11-1583-2019>
- Chabot, D., Stapleton, S., & Francis, C. M. (2022). Using Web images to train a deep neural network to detect sparsely distributed wildlife in large volumes of remotely sensed imagery: A case study of polar bears on sea ice. *Ecological Informatics*, 68, 101547. <https://doi.org/10.1016/J.ECOINF.2021.101547>
- CHEN, H., Oguchi, T., & WU, P. (2017). Assessment for soil loss by using a scheme of alternative sub-models based on the RUSLE in a Karst Basin of Southwest China.



- Journal of Integrative Agriculture*, 16(2), 377–388. [https://doi.org/10.1016/S2095-3119\(16\)61507-1](https://doi.org/10.1016/S2095-3119(16)61507-1)
- de Brogniez, D., Ballabio, C., Stevens, A., Jones, R. J. A., Montanarella, L., & van Wesemael, B. (2015). A map of the topsoil organic carbon content of Europe generated by a generalized additive model. *European Journal of Soil Science*, 66(1), 121–134.
- Demirci, A., & Karaburun, A. (2012). Estimation of soil erosion using RUSLE in a GIS framework: A case study in the Buyukcekmece Lake watershed, northwest Turkey. *Environmental Earth Sciences*, 66(3), 903–913. <https://doi.org/10.1007/s12665-011-1300-9>
- Didan, K., Munoz, A. B., Solano, R., & Huete, A. (2015). *MODIS Vegetation Index User's Guide (MOD13 Series) Version 3.0 Ccollection 6*. 2015(May), 38.
- Durigon, V. L., Carvalho, D. F., Antunes, M. A. H., Oliveira, P. T. S., & Fernandes, M. M. (2014). NDVI time series for monitoring RUSLE cover management factor in a tropical watershed. *International Journal of Remote Sensing*, 35(2), 441–453. <https://doi.org/10.1080/01431161.2013.871081>
- ESRI. (2013). The Language of Spatial Analysis. *Esri*, 36(June), 1–49.
- Esser, K., Vågen, T. G., Tilahun, Y., & Haile, M. (2002). Soil conservation in Tigray. *Soil Conservation*, 5, 1–21.
- Evans, R., & Boardman, J. (2016). The new assessment of soil loss by water erosion in Europe. Panagos P. et al., 2015 *Environmental Science & Policy* 54, 438–447-A response. *Environmental Science and Policy*, 58, 11–15. <https://doi.org/10.1016/j.envsci.2015.12.013>
- Fiener, P., Neuhaus, P., & Botschek, J. (2013). Long-term trends in rainfall erosivity-analysis of high resolution precipitation time series (1937–2007) from Western Germany. *Agricultural and Forest Meteorology*, 171–172, 115–123. <https://doi.org/10.1016/j.agrformet.2012.11.011>
- Filho, W. L., & de Trinchiera Gomez, J. (2017). Rainwater-smart agriculture in arid and semi-arid areas: Fostering the use of rainwater for food security, poverty alleviation, landscape restoration and climate resilience. *Rainwater-Smart Agriculture in Arid and Semi-Arid Areas: Fostering the Use of Rainwater for Food Security, Poverty Alleviation, Landscape Restoration and Climate Resilience*, December, 1–392. <https://doi.org/10.1007/978-3-319-66239-8>
- Fitsum, H., John, P., & Nega, G. (2000). Land degradation in the Highlands of Tigray and Strategies for Sustainable Land Management. *Policies for Sustainable Land Management in the Highlands of Ethiopia*, 30(July 1999), 2–75.
- Ganasri, B. P., & Ramesh, H. (2016). Assessment of soil erosion by RUSLE model using remote sensing and GIS - A case study of Nethravathi Basin. *Geoscience Frontiers*, 7(6), 953–961. <https://doi.org/10.1016/j.gsf.2015.10.007>
- Gebregziabher, et al. (2009). Contour furrows for in situ soil and water conservation, Tigray, Northern Ethiopia. *Soil and Tillage Research*, 103(2), 257–264. <https://doi.org/10.1016/j.still.2008.05.021>
- Ghosal, K., & Das Bhattacharya, S. (2020). A Review of RUSLE Model. *Journal of the Indian Society of Remote Sensing*, 48(4), 689–707. <https://doi.org/10.1007/s12524-019-01097-0>
- Govers, G., & Moeyersons, J. (2005). Effectiveness of stone bunds in controlling soil erosion on cropland in the Tigray Highlands, northern Ethiopia. 287–297. <https://doi.org/10.1079/SUM2005321>

- Hateffard, F., Mohammed, S., Alsafadi, K., Enaruvbe, G. O., Heidari, A., Abdo, H. G., & Rodrigo-Comino, J. (2021). CMIP5 climate projections and RUSLE-based soil erosion assessment in the central part of Iran. *Scientific Reports*, *11*(1). <https://doi.org/10.1038/S41598-021-86618-Z>
- He, Y., Wang, L., Niu, Z., & Nath, B. (2022). Vegetation recovery and recent degradation in different karst landforms of southwest China over the past two decades using GEE satellite archives. *Ecological Informatics*, *68*, 101555. <https://doi.org/10.1016/J.ECOINF.2022.101555>
- K., K., F., B., & O., O. (2020). Assessment of Soil Erosion By Rusle Model Using Gis: a Case Study of Chemorah Basin, Algeria. *Malaysian Journal of Geosciences*, *4*(2), 70–78. <https://doi.org/10.26480/mjg.02.2020.70.78>
- Kinnell, P. I. A. (2014). Applying the RUSLE and the USLE-M on hillslopes where runoff production during an erosion event is spatially variable. *Journal of Hydrology*, *519*(PD), 3328–3337. <https://doi.org/10.1016/j.jhydrol.2014.10.016>
- Kaygusuz, K. (2011). Energy services and energy poverty for sustainable rural development. *Renewable and Sustainable Energy Reviews*, *15*(2), 936–947. <https://doi.org/10.1016/j.rser.2010.11.003>
- Kouli, M., Soupios, P., & Vallianatos, F. (2009). Soil erosion prediction using the Revised Universal Soil Loss Equation (RUSLE) in a GIS framework, Chania, Northwestern Crete, Greece. *Environmental Geology*, *57*(3), 483–497. <https://doi.org/10.1007/s00254-008-1318-9>
- Kuria, A. W., Barrios, E., Pagella, T., Muthuri, C. W., Mukuralinda, A., & Sinclair, F. L. (2018). Farmers' knowledge of soil quality indicators along a land degradation gradient in Rwanda. *Geoderma Regional*, December, e00199. <https://doi.org/10.1016/j.geodrs.2018.e00199>
- Liu, K., Tang, G., Jiang, L., Zhu, A. X., Yang, J., & Song, X. (2015). Regional-scale calculation of the LS factor using parallel processing. *Computers and Geosciences*, *78*, 110–122. <https://doi.org/10.1016/j.cageo.2015.02.001>
- Lu, D., Li, G., Valladares, G. S., & Batistella, M. (2004). Mapping soil erosion risk in Rondônia, Brazilian Amazonia: Using RUSLE, remote sensing and GIS. *Land Degradation and Development*, *15*(5), 499–512. <https://doi.org/10.1002/ldr.634>
- Luvai, A., Obiero, J., & Omuto, C. (2022). Soil Loss Assessment Using the Revised Universal Soil Loss Equation (RUSLE) Model. *Applied and Environmental Soil Science*, 2022. <https://doi.org/10.1155/2022/2122554>
- Mitasova, H., Barton, M., Ullah, I., Hofierka, J., & Harmon, R. S. (2013). GIS-Based Soil Erosion Modeling. In *Treatise on Geomorphology* (Vol. 3, Issue November 2017). <https://doi.org/10.1016/B978-0-12-374739-6.00052-X>
- Megerssa, G. R., & Bekere, Y. B. (2019). Causes, consequences and coping strategies of land degradation: Evidence from Ethiopia. *Journal of Degraded and Mining Lands Management*, *7*(1), 1953–1957. <https://doi.org/10.15243/jdmlm.2019.071.1953>
- Mekuria, W., Veldkamp, E., Haile, M., Gebrehiwot, K., Muys, B., & Nyssen, J. (2009). Effectiveness of exclosures to control soil erosion and local community perception on soil erosion in Tigray, Ethiopia. *African Journal of Agricultural Research*, *4*(4), 365–377.
- Moges, D. M., & Bhat, H. G. (2017). Integration of geospatial technologies with RUSLE for analysis of land use/cover change impact on soil erosion: case study in Rib

- watershed, north-western highland Ethiopia. *Environmental Earth Sciences*, 76(22), 1–14. <https://doi.org/10.1007/s12665-017-7109-4>
- Nyssen, J., Clymans, W., Descheemaeker, K., Poesen, J., Vandecasteele, I., Vanmaercke, M., Zenebe, A., Van Camp, M., Haile, M., Haregeweyn, N., Moeyersons, J., Martens, K., Gebreyohannes, T., Deckers, J., & Walraevens, K. (2010). Impact of soil and water conservation measures on catchment hydrological response—a case in north Ethiopia. *Hydrological Processes*, 24(13), 1880–1895. <https://doi.org/10.1002/hyp.7628>
- Okoye, C. U. (1998). Comparative analysis of factors in the adoption of traditional and recommended soil erosion control practices in N. *Soil and Tillage Research*, 45(3–4), 251–263. [https://doi.org/10.1016/S0933-3630\(96\)00137-7](https://doi.org/10.1016/S0933-3630(96)00137-7)
- Panagos, P., Meusburger, K., Ballabio, C., Borrelli, P., & Alewell, C. (2014). Soil erodibility in Europe: A high-resolution dataset based on LUCAS. *Science of the Total Environment*, 479–480(1), 189–200. <https://doi.org/10.1016/j.scitotenv.2014.02.010>
- P.U., I., A.A., O., O.C., C., I.I., E., & M.M., M. (2017). Soil Erosion: A Review of Models and Applications. *International Journal of Advanced Engineering Research and Science*, 4(12), 138–150. <https://doi.org/10.22161/ijaers.4.12.22>
- Rockström, J., & Falkenmark, M. (2015). Agriculture: Increase water harvesting in Africa. *Nature*, 519(7543), 283–285. <https://doi.org/10.1038/519283a>
- Schmidt, S., Tresch, S., & Meusburger, K. (2019). Modification of the RUSLE slope length and steepness factor (LS-factor) based on rainfall experiments at steep alpine grasslands. *MethodsX*, 6, 219–229. <https://doi.org/10.1016/j.mex.2019.01.004>
- Sileshi, M., Kadigi, R., Mutabazi, K., & Sieber, S. (2019). Determinants for adoption of physical soil and water conservation measures by smallholder farmers in Ethiopia. *International Soil and Water Conservation Research*, 7(4), 354–361. <https://doi.org/10.1016/j.iswcr.2019.08.002>
- Tanyaş, H., Kolat, Ç., & Süzen, M. L. (2015). A new approach to estimate cover-management factor of RUSLE and validation of RUSLE model in the watershed of Kartalkaya Dam. *Journal of Hydrology*, 528, 584–598. <https://doi.org/10.1016/j.jhydrol.2015.06.048>
- Tadesse, A., Gebrelibanos, T., & Geberehiwot, M. (2016). Characterization and Impact Assessment of Water Harvesting Techniques : A Case Study of Abreha Weatsbeha Watershed , Tigray , Ethiopia . 1–28.
- Teka, K., Haftu, M., Ostwald, M., & Cederberg, C. (2020). Can integrated watershed management reduce soil erosion and improve livelihoods? A study from northern Ethiopia. *International Soil and Water Conservation Research*, 8(3), 266–276. <https://doi.org/10.1016/j.iswcr.2020.06.007>
- Tesfahunegn, G. B., & Gebru, T. A. (2020). Variation in soil properties under different cropping and other land-use systems in Dura catchment, Northern Ethiopia. *PloS one*, 15(2), e0222476.
- Tian, P., Zhu, Z., Yue, Q., He, Y., Zhang, Z., Hao, F., Guo, W., Chen, L., & Liu, M. (2021). Soil erosion assessment by RUSLE with improved P factor and its validation: Case study on mountainous and hilly areas of Hubei Province, China. *International Soil and Water Conservation Research*, 9(3), 433–444. <https://doi.org/10.1016/j.iswcr.2021.04.007>
- Tomislav Hengl, & Ichsani Wheeler. (2018). Soil organic carbon content in x 5 g / kg at 6 standard depths (0, 10, 30, 60, 100 and 200 cm) at 250 m resolution (Version v02) [Data set]. Zenodo. 10.5281/zenodo.1475457
- Van Remortel, R. D., Hamilton, M. E., & Hickey, R. J. (2001). Estimating the LS factor for RUSLE through iterative slope length processing of digital elevation data within

- arclInfo grid. *Cartography*, 30(1), 27–35.  
<https://doi.org/10.1080/00690805.2001.9714133>
- Vancampenhout, K., Nyssen, J., Gebremichael, D., Deckers, J., Poesen, J., Haile, M., & Moeyersons, J. (2006). Stone bunds for soil conservation in the northern Ethiopian highlands: Impacts on soil fertility and crop yield. *Soil and Tillage Research*, 90(1–2), 1–15. <https://doi.org/10.1016/j.still.2005.08.004>
- Vatandaşlar, C., & Yavuz, M. (2017). Modeling cover management factor of RUSLE using very high-resolution satellite imagery in a semiarid watershed. *Environmental Earth Sciences*, 76(2). <https://doi.org/10.1007/s12665-017-6388-0>
- Waters, N. (2012). A Review of “Handbook of Applied Spatial Analysis: Software Tools, Methods and Applications.” In *Annals of the Association of American Geographers* (Vol. 102, Issue 1). <https://doi.org/10.1080/00045608.2011.624965>
- Wu, T. Y., Yeh, K. T., Hsu, H. C., Yang, C. K., Tsai, M. J., & Kuo, Y. F. (2022). Identifying Fagaceae and Lauraceae species using leaf images and convolutional neural networks. *Ecological Informatics*, 68, 101513. <https://doi.org/10.1016/J.ECOINF.2021.101513>
- Xu, L., Xu, X., & Meng, X. (2013). Risk assessment of soil erosion in different rainfall scenarios by RUSLE model coupled with Information Diffusion Model: A case study of Bohai Rim, China. *Catena*, 100, 74–82. <https://doi.org/10.1016/j.catena.2012.08.012>
- Yue, T., Xie, Y., Yin, S., Yu, B., Miao, C., & Wang, W. (2020). Effect of time resolution of rainfall measurements on the erosivity factor in the USLE in China. *International Soil and Water Conservation Research*, 8(4), 373–382. <https://doi.org/10.1016/j.iswcr.2020.06.001>
- Zerssa, G., Feyssa, D., Kim, D., & Eichler-löbermann, B. (2021). Challenges of Smallholder Farming in Ethiopia and Opportunities by Adopting Climate-Smart Agriculture. 1–25.

# Appendix I

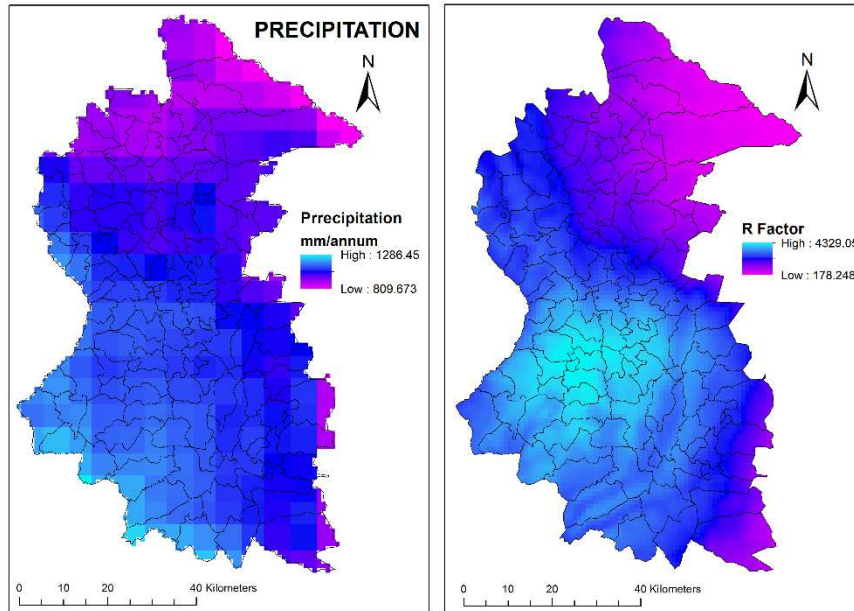


Figure 3 Erosivity factor R

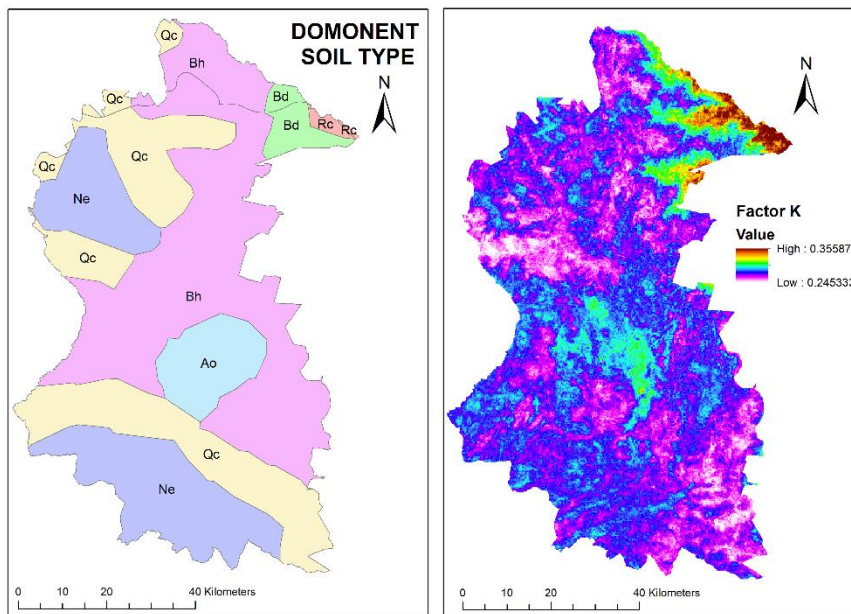
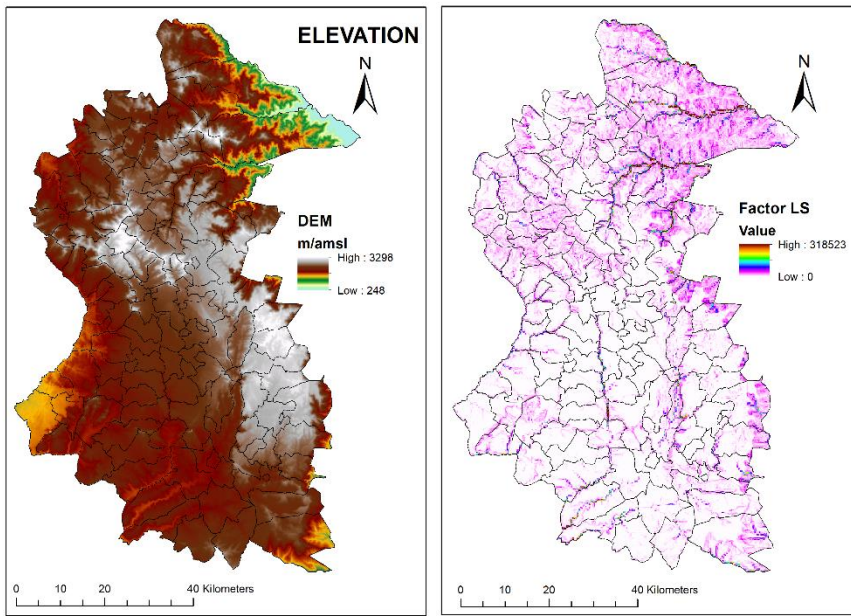
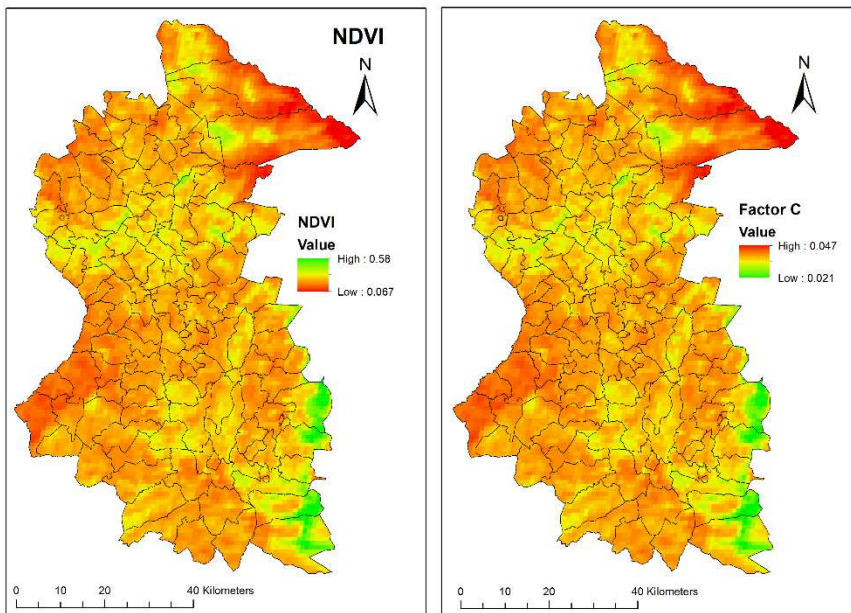


Figure 4 Erosivity factor K



*Figure 5 Erosivity factor LS*



*Figure 6 Erosivity factor C*

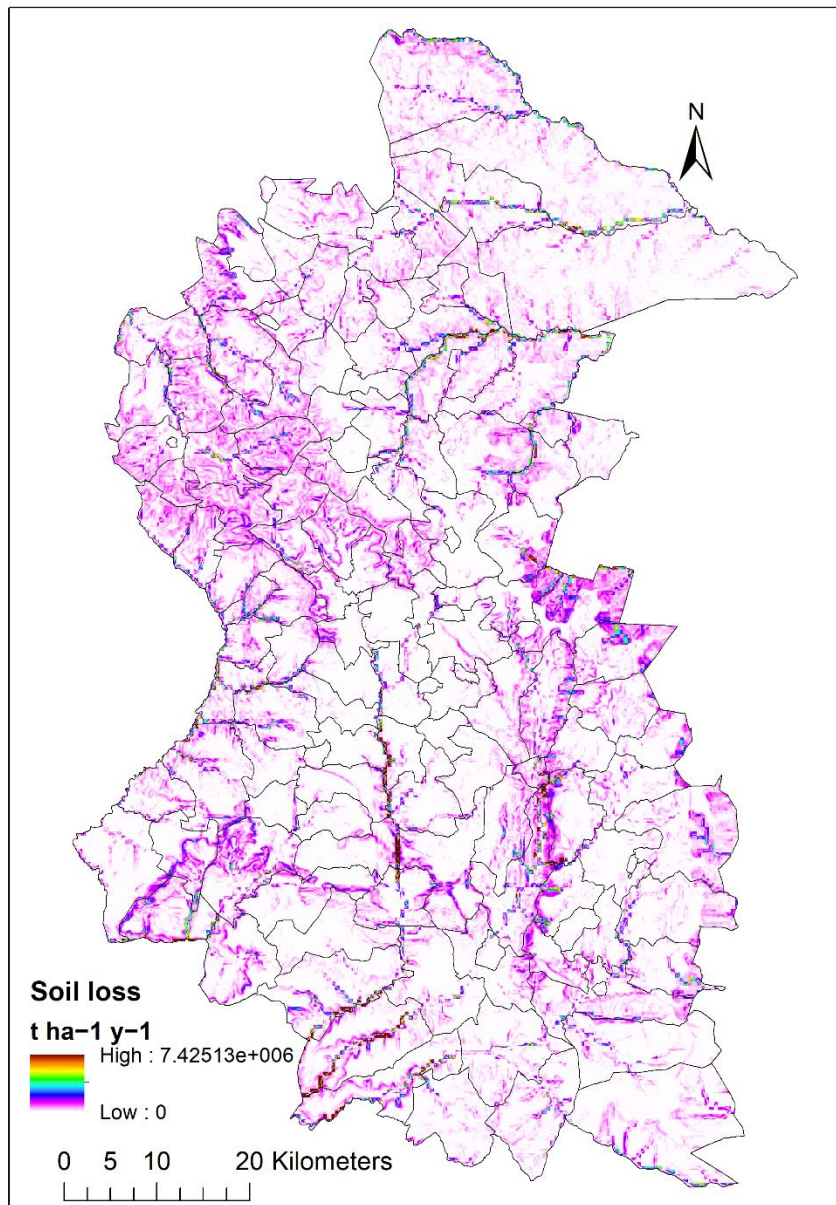


*Figure 7 Estimated Annual soil erosion*

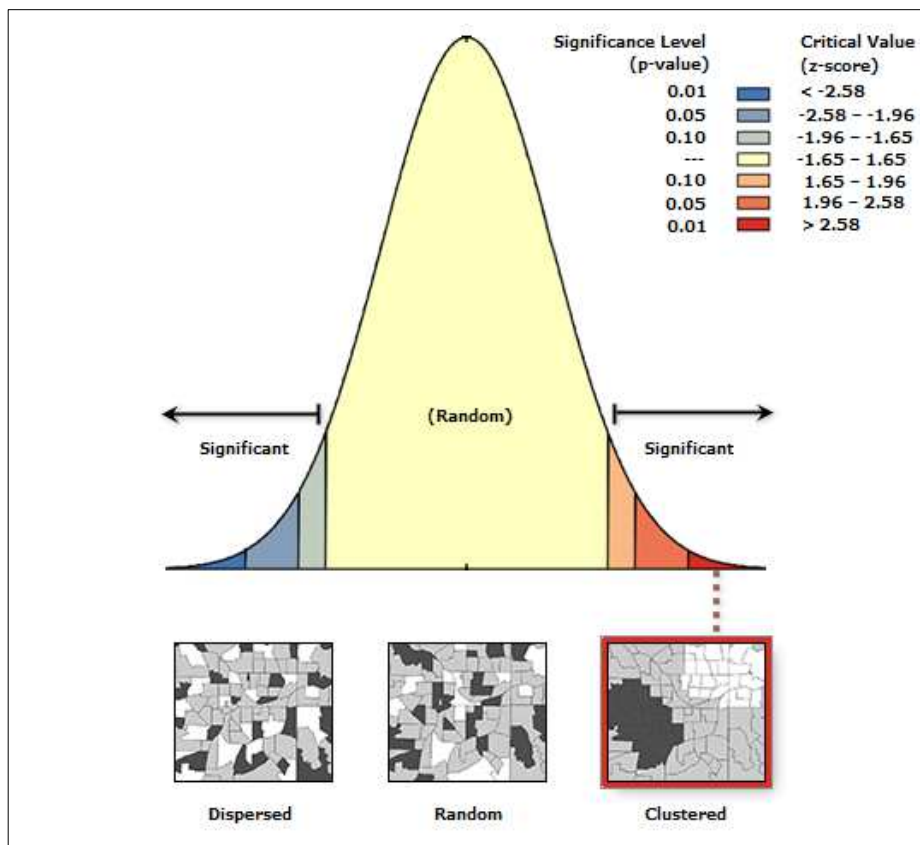


Figure 8 Pattern at Kebele level

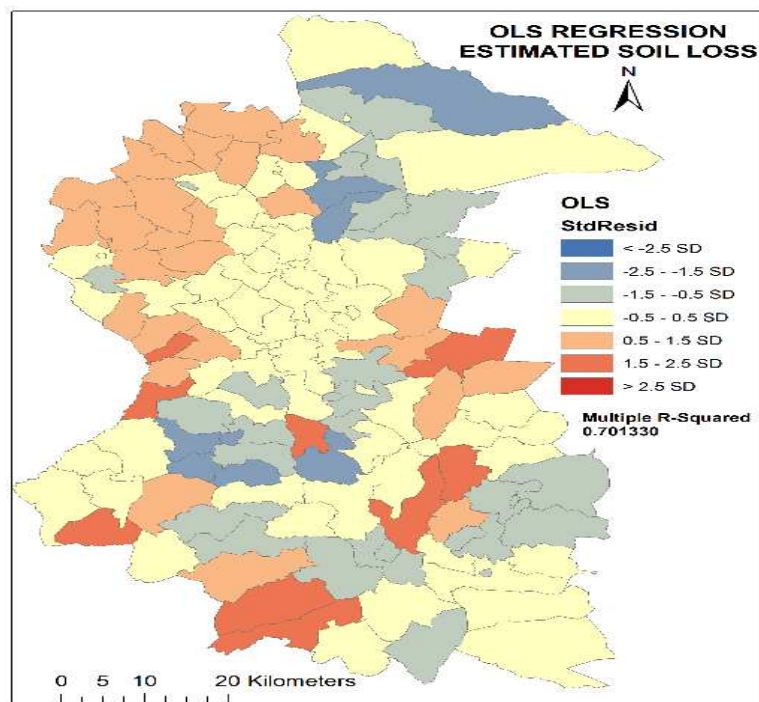
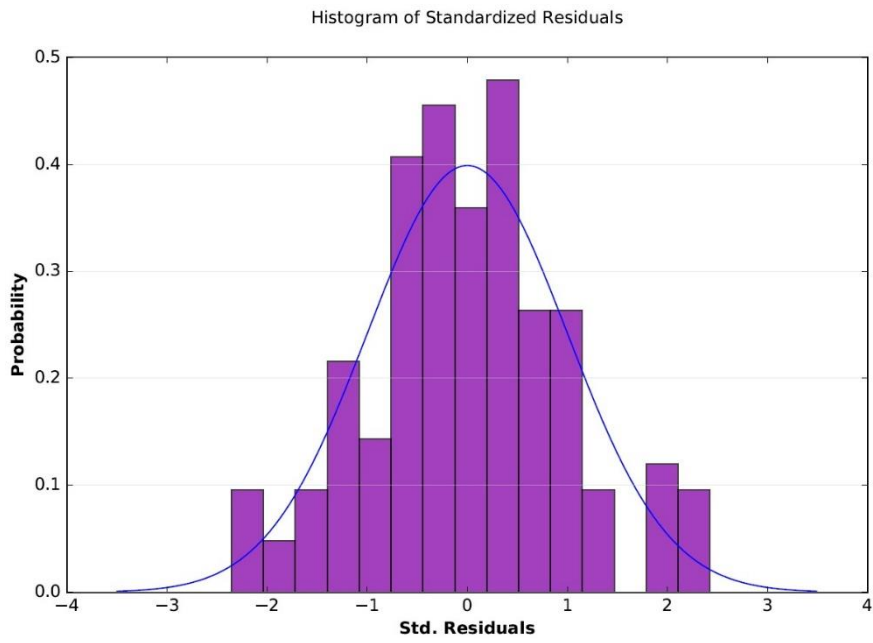


Figure 9 Standard Residual Map





*Figure 10 Histogram of residuals*

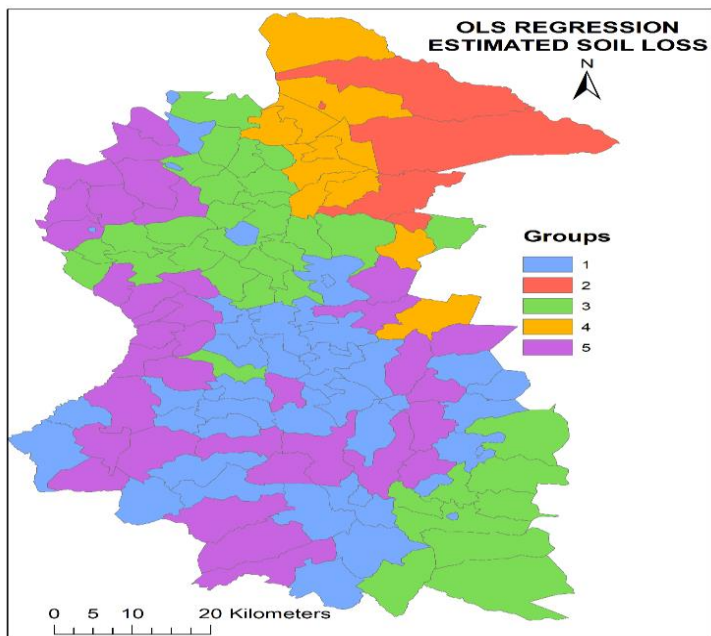


Figure 11 Groups of Annual soil loss Prediction

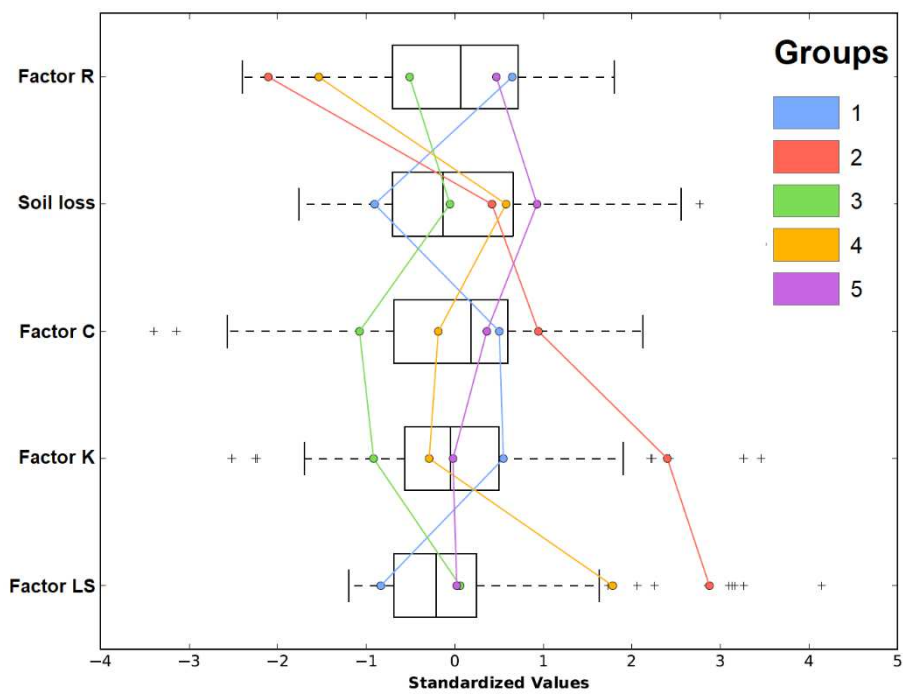


Figure 12 Parallel Box Plot



Figure 13 Groups based on mean soil loss

Dataset	Content	Format	Data Source
Precipitation	Monthly Rainfall in mm, one km spatial resolution, Covering Period 2007-2018.	tif	<a href="https://openlandmap.org/">https://openlandmap.org/</a> (Brocca et al., 2019)
Soil	Sand, Silt, Clay, Organic Content	tif	<a href="https://openlandmap.org/">https://openlandmap.org/</a>
DEM	SRTM dataset with 1 km spatial resolution	tif	<a href="https://www.hydrosheds.org/">https://www.hydrosheds.org/</a>
NDVI	The MODIS vegetation index (VI) products.	tif	<a href="https://lpdaac.usgs.gov/">https://lpdaac.usgs.gov/</a>
Basic geographical information	Administrative Map	Vector	<a href="https://www.diva-gis.org/gdata">https://www.diva-gis.org/gdata</a>

Moran's Index:	0.148521
Expected Index:	-0.007692
Variance:	0.001568
z-score:	3.944822
p-value:	0.000080

Variable	Coefficient	Std Error	t-Statistic	Probability	Robust_SE	Robust_t	Robust_Pr	VIF
Intercept	446729.83	78704.50	5.67	0.000	71907.48	6.212	0.000000*	-----
C	940082.00	1159673.5	0.81	0.4190	1041922.70	0.902	0.368633	1.52001
K	-1961511.5	347615.20	-5.64	0.000	329113.78	-5.95998	0.000000*	1.458368
LS	15.03751	0.905789	16.60	0.000	1.240123	12.125	0.000000*	1.912069
R	25.58718	2.279686	11.22	0.000	2.562404	9.98562	0.000000*	1.952451

Table 04 OLS Diagnostics			
Input Features:	Kebele	Dependent Variable:	Est. Soil Loss Mean
No. of Observations:	131	Akaike's Information Criterion (AICc)	2930.81
Multiple R-Squared:	0.701	Adjusted R-Squared	0.69
Joint F-Statistic:	73.968	Prob(>F), (4659)	0.000000*
Joint Wald Statistic:	177.372	Prob(>chi-squared), (4)	0.000000*
Koenker (BP) Statistic:	42.608	Prob(>chi-squared), (4)	0.000000*
Jarque-Bera Statistic:	0.488	Prob(>chi-squared), (2)	0.784